Preprints.org

Article

Not peer-reviewed version

A Class of Efficient Sixth-Order Iterative Methods for Solving the Nonlinear Shear Model of a Reinforced Concrete Beam

José Javier Padilla , Francisco I. Chicharro , Alicia Cordero , Alejandro M. Hernández-Díaz ,
Juan R. Torregrosa *

Posted Date: 3 January 2024

doi: 10.20944/preprints202401.0149.v1

Keywords: Nonlinear systems; iterative methods; reinforced concrete; shear behaviour; stability; convergence order; efficiency

Preprints.org (www.preprints.org) | NOT PEER-REVIEWED | Posted: 3 January 2024 doi:10.20944/preprints202401.0149.v1

Article

A Class of Efficient Sixth-Order Iterative Methods for Solving the Nonlinear Shear Model of a Reinforced Concrete Beam

José J. Padilla [1], Francisco I. Chicharro [2], Alicia Cordero [2], Alejandro M. Hernández-Díaz [3] and Juan R. Torregrosa [2,*]

[1] Departamento de Ingeniería Civil, UCAM Universidad Católica de Murcia, 30107 Guadalupe, Spain; jjpadilla@ucam.edu
[2] Instituto Universitario de Matemàtica Multidisciplinar, Universitat Politècnica de València, 46022 València, Spain; frachilo@mat.upv.es (F.I.C.); acordero@mat.upv.es (A.C.)
[3] Área de Mecánica de Medios Continuos y Teoría de Estructuras, Universidad de La Laguna, 38200 La Laguna, Spain; ahernadi@ull.edu.es
* Correspondence: jrtorre@mat.upv.es

Abstract: In this paper, we present a three-step sixth-order iterative schemes to estimate the solutions of a nonlinear systems of equations, for predicting the shear strength of a reinforced concrete beam. This procedure is designed by means of a weight function technique. The values for the parameters of this system were randomly selected inside the prescribed ranges by technical standards for structural concrete; moreover, some of this parameters were fixed taking into consideration the solvability region of the adopted steel constitutive model. The efficiency of the new class is compared with other current schemes, with very good results.

Keywords: nonlinear systems; iterative methods; reinforced concrete; shear behaviour; stability; convergence order; efficiency

---

1. Introduction

Reinforced and prestressed concrete beams represent a structural type that resists internal stresses in a relatively complex manner due to their constitutive nature. Prior to cracking of the concrete, the shear loads are carried by a set of diagonal compressive stresses complemented by another set of diagonal tensile stresses acting perpendicular to the first ones. Once the concrete tensile strength is reached, cracks form in the direction normal to the diagonal tensile stresses while preexisting cracks spread and change inclination. Then the ability of concrete to transmit diagonal tensile stresses is significantly reduced and the appropriate reinforcement is necessary to create a new system of internal stresses that carry the shear acting on the beam after cracking. Shear design procedures for reinforced concrete that determine the inclination of such cracks by considering the strains in the diagonally stressed concrete, as well as in the longitudinal and transverse reinforcement, are known as Compression Field Theories (CFT) [1,2].

As justified at Section 2, CFT mechanical models involve several types of nonlinearities, among other reasons, due to the constitutive relationships of the reinforced concrete. The implementation of these models usually requires the application of numerical methods for solving the corresponding nonlinear equations, such as, for example, Newton-type methods [3]. In fact, the correct solver for solving a nonlinear problem is often a choice between computational cost and accuracy [4–7]. Moreover, in this work the previous determination of a solvability region using algebraic procedures is also necessary in order to improve the efficiency of the numerical solver, as indicated at Section 2.

Solving systems of nonlinear equations is an important problem in science and engineering. The objective is to find the roots of the nonlinear system $F(x) = 0$, being F a multidimensional function, $F : D \subseteq \mathbb{R}^n \to \mathbb{R}^n$, on D convex set , of size $n \times n$, $F(x) = (f_1(x), f_2(x), \dots, f_n(x))^T$, being f_i, $i = 1, 2, \dots, n$, the functional coordinates of F.

Preprints.org (www.preprints.org) | NOT PEER-REVIEWED | Posted: 3 January 2024 doi:10.20944/preprints202401.0149.v1

One of the most commonly used methods, is the classical Newton method, which has a quadratic order of convergence and iterative expression

$$x^{(k+1)} = x^{(k)} - [F'(x^{(k)})]^{-1}F(x^{(k)}), \quad k = 0, 1, 2, \ldots, \tag{1}$$

where $F'(x^{(k)})$ is a Jacobian matrix of F at k-th iteration.

Several Newton type procedures, by using different techniques, have been published in the last years. Their main aim is accelerating the convergence or increasing their efficiency. In the last section we are going to recall some of them, for comparison purposes.

All the schemes we are going to mention use, in their iterative expression, the Jacobian matrix of function F and have, under the usual conditions, convergence order 6. We will compare these methods, from the point of view of results, convergence order and computational efficiency, with the methods proposed in this paper that also have order 6 and use $F'(x)$ in their expressions.

In [8], by using the weight function procedure, the authors designed a Jarratt-type method for solving nonlinear systems, denoted by $M2_6$, whose iterative expression is:

$$\left\{ \begin{array}{lcl} y^{(k)} & = & x^{(k)} - \frac{2}{3}[F'(x^{(k)})]^{-1}F(x^{(k)}),\ k = 0, 1, \ldots \\ z^{(k)} & = & x^{(k)} - \left(\frac{5}{8}I + \frac{3}{8}([F'(y^{(k)})]^{-1}F'(x^{(k)}))^2\right)[F'(x^{(k)})]^{-1}F(x^{(k)}), \\ x^{(k+1)} & = & z^{(k)} - \left(\frac{-9}{4}I - \frac{15}{8}[F'(x^{(k)})]^{-1}F'(y^{(k)}) + \frac{11}{8}[F'(y^{(k)})]^{-1}F'(x^{(k)})\right)[F'(y^{(k)})]^{-1}F(z^{(k)}), \end{array} \right. \tag{2}$$

where I denotes the identity matrix of size $n \times n$. This method needs to evaluate the Jacobian matrix in two points and uses two inverse operators. These elements increase the number of operations per iteration.

In order to reduce the number of inverse operators, Narang et al. in [9] from a Chebyshev-Halley-type family, constructed a class of iterative schemes of sixth-order, one of its members denoted by $M_{6,2}(1/2, 0)$ has the following iterative expression:

$$\left\{ \begin{array}{lcl} y^{(k)} & = & x^{(k)} - \frac{2}{3}[F'(x^{(k)})]^{-1}F(x^{(k)}), \\ z^{(k)} & = & x^{(k)} - \left(\frac{1}{2}G(x^{(k)})\right)H(G(x^{(k)}))[F'(x^{(k)})]^{-1}F(x^{(k)}), \\ x^{(k+1)} & = & z^{(k)} - \left(I + \frac{3}{2}G(x^{(k)})\right)[F'(x^{(k)})]^{-1}F(z^{(k)}),\ k = 0, 1, \ldots \end{array} \right. \tag{3}$$

where $G(x^{(k)}) = I - [F'(x^{(k)})]^{-1}F'(y^{(k)})$ and $H(G(x^{(k)})) = I - \frac{1}{4}G(x^{(k)}) + \frac{11}{8}(G(x^{(k)}))^2$.

Behl et al. in [10], using the indeterminate parameter procedure, designed a family of iterative sixth-order methods for solving systems of nonlinear equations, one of whose members, denoted by PM1, has the iterative expression

$$\left\{ \begin{array}{lcl} y^{(k)} & = & x^{(k)} - \frac{2}{3}[F'(x^{(k)})]^{-1}F(x^{(k)}), \\ z^{(k)} & = & y^{(k)} - \left(4I - 3[F'(x^{(k)})]^{-1}F'(y^{(k)}) + \frac{9}{8}([F'(x^{(k)})]^{-1}F'(y^{(k)}))^{-2}\right)[F'(x^{(k)})]^{-1}F(x^{(k)}), \\ x^{(k+1)} & = & z^{(k)} - \left(\frac{5}{2}I - \frac{3}{2}[F'(x^{(k)})]^{-1}F'(y^{(k)})\right)[F'(x^{(k)})]^{-1}F(z^{(k)}),\ k = 0, 1, \ldots \end{array} \right. \tag{4}$$

Finally, Yaseen and Zafar presented in [11] a Jarratt-type scheme of three-steps for solving nonlinear systems, denoted by $FS6$, with sixth-order convergence and iterative expression

$$\left\{ \begin{array}{lcl} y^{(k)} & = & x^{(k)} - \frac{2}{3}[F'(x^{(k)})]^{-1}F(x^{(k)}), \\ z^{(k)} & = & x^{(k)} - \left(\frac{5}{8}[U_k]^{-1} + \frac{3}{8}U_k\right)[F'(y^{(k)})]^{-1}F(x^{(k)}), \\ x^{(k+1)} & = & z^{(k)} - \left(\frac{-13}{2}I + \frac{9}{2}[V_k]^{-1} + 3V_k\right)[F'(x^{(k)})]^{-1}F(z^{(k)}),\ k = 0, 1, \ldots, \end{array} \right. \tag{5}$$

where $U_k = [F'(y^{(k)})]^{-1}F'(x^{(k)})$ and $V_k = [F'(x^{(k)})]^{-1}F'(y^{(k)})$.

The rest of the paper is organized as follows. In Section 2, we describe the nonlinear system obtained for predicting the shear strength of a reinforced concrete beam. The efficient method for estimating its solution is presented in Section 3, as well as its convergence order.

Preprints.org (www.preprints.org) | NOT PEER-REVIEWED | Posted: 3 January 2024 doi:10.20944/preprints202401.0149.v1

2. Problem statement

In [1], the authors proposed this stress-strain relationship for concrete cracked in tension:

$$\sigma_1 = \begin{cases} E_c \varepsilon_1, & \varepsilon_1 \leq \varepsilon_{ct}, \\ \dfrac{\alpha f_{ct}}{1 + \sqrt{500\varepsilon_1}}, & \varepsilon_1 > \varepsilon_{ct}, \end{cases} \tag{6}$$

where σ_1 represents the contribution of tensile stresses in the concrete between the cracks or tension stiffening effect, ε_1 is the principal tensile strain, being E_c the modulus of elasticity of the concrete, ε_{ct} the strain related to the strength of the tensile, f_{ct}. Coefficient α is equal to 1.0 in case of fast and non-cyclic loads and for deformed bars.

Regarding to the concrete behaviour in compression, Vecchio and Collins formulated in [12], inside the Modified Compression Field Theory (MCFT), the following relationship between diagonal compressive strain, ε_2 and the diagonal (or principal) compressive stress, σ_2:

$$\begin{aligned} &\sigma_2 = f_{2max} \left[2 \left(\frac{\varepsilon_2}{\varepsilon_c} \right) - \left(\frac{\varepsilon_2}{\varepsilon_c} \right)^2 \right], \\ &\text{with } \; f_{2max} = \frac{f_c}{0.8+170\varepsilon_1} \leq f_c, \end{aligned} \tag{7}$$

where ε_c is the compressive strain related to the compressive strength of concrete in a cylinder test f_c, ε_1 is the coexisting principal tensile strain, and f_{2max} is the maximum compressive stress in a diagonally cracked web.

In CFT procedures, perfect bond between concrete and steel is assumed; in consequence, any deformation developed by the reinforcement is identical to the one experienced by the surrounding concrete in the same direction; thus, a single average strain tensor of the composite material is adopted. The following relationship is considered by compatibility of the strains in the reinforcement and the diagonally stressed concrete:

$$\tan^2\theta = \frac{\varepsilon_x - \varepsilon_2}{\varepsilon_t - \varepsilon_2} = \frac{\varepsilon_1 - \varepsilon_t}{\varepsilon_1 - \varepsilon_x}, \tag{8}$$

where ε_x is the mean longitudinal strain and ε_t is the mean transversal strain on the web of a beam oriented according to the orthogonal $x - t$ directions (see Figure 1). The strain ε_2 is aligned in the direction of the compressive struts, at angle θ to the longitudinal axis (x) of the beam. Moreover, due to strain tensor, the main tensile strain is

$$\varepsilon_1 = \varepsilon_x + \varepsilon_t + \varepsilon_2, \tag{9}$$

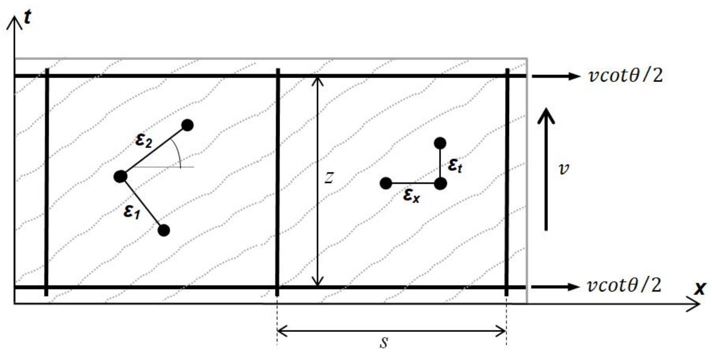

Figure 1. Strain compatibility between diagonally stressed concrete and the reinforcement in the cracked web of a reinforced concrete beam

Preprints.org (www.preprints.org) | NOT PEER-REVIEWED | Posted: 3 January 2024 doi:10.20944/preprints202401.0149.v1

On the other hand, in CFT models the equilibrium between the external loads and the internal forces is governed by the following equations:

$$\sigma_2 = \frac{v}{b_w z}(\tan\theta + \cot\theta) - \sigma_1, \tag{10}$$

$$2A_{st}\sigma_{st} = (\sigma_2 \sin^2\theta - \sigma_1 \cos^2\theta) b_w s, \tag{11}$$

$$4A_{sx}\sigma_{sx} + A_p\sigma_p = (\sigma_2 \cos^2\theta - \sigma_1 \sin^2\theta) b_w z = \frac{v}{\tan\theta} - \sigma_1 b_w z, \tag{12}$$

where θ is the angle of the main tensile stress, z is the flexural lever arm, s is the stirrup spacing, v is the internal shear force, and b_w is the web width; A_{sx}, A_{st} and A_p are the cross-section surfaces for the longitudinal bars, the stirrup legs and the prestressed reinforcement, respectively, and σ_{sx}, σ_{st} and σ_p are the related mean tensile stresses. The angles of inclination of principal strains coincide with the angles of inclination of principal stresses; this is known as EPA assumption or as Wagner's hypothesis [2,13].

The main difference among CFT methods lies in the treatment of the steel behavior [12,14,15]. In this work one of the most recent approaches to the steel behaviour is adopted, the so-called Refined Compression Field Theory (RCFT) [15,16], which is based on the concept of an embedded bar model that takes into account the concrete tension stiffening effect between cracks. This last theory allows us to implement, in the most general case, the following average stress-strain model for each kind of steel reinforcement in the beam (that is, the transverse stirrups and the longitudinal reinforcement):

$$\sigma_{s,i} = \begin{cases} f_{y,i} - \frac{A_{c,i}}{A_{s,i}} \frac{f_{ct}}{1+\sqrt{3.6 M_i \varepsilon_{s,i}}} & \text{if} \quad \varepsilon_{s,i} \geq \varepsilon_{max,i}, \\ E_s \varepsilon_{s,i} & \text{if} \quad \varepsilon_{s,i} < \varepsilon_{max,i}, \end{cases}$$

$$i \in \{x, t\}, \text{ and in which} \tag{13}$$

$$\varepsilon_{max,i} = \frac{f_{y,i}}{E_s} - \frac{\frac{A_{c,i} f_{ct}}{1+\sqrt{3.6 M_i \varepsilon_{max,i}}}}{E_s A_{s,i}},$$
$$M_i = \frac{A_{c,i}}{\sum \pi \phi_i},$$

where the subscripts x and t refer to the longitudinal and the transverse reinforcement, respectively (then, expression (13) actually involves two equations); f_y is the steel yield stress, E_s is the elastic modulus of the steel, $\sigma_{s,av}$ is the average tensile stress in the steel, $\varepsilon_{s,av}$ is the average strain in the reinforcing bar, $\varepsilon_{max,i}$ is the apparent yield strain (cf. [15]), A_s is the cross-section of the longitudinal or transverse steel bars, M is the bond parameter and A_c is the area of concrete bonded to the bar playing in the tension stiffening effect (that usually is considered equal to the rectangular surface around the bar and on a distance not exceeding 7.5ϕ from its center, where ϕ is the diameter of the bar).

In case of prestressed concrete elements, the following two more equations are needed:

$$\varepsilon_p = \varepsilon_x + \Delta\varepsilon_p, \tag{14}$$

$$\sigma_p = \begin{cases} E_p \varepsilon_p & , \quad \varepsilon_p \leq \frac{f_{yp}}{E_p}, \\ f_{yp} & , \quad \varepsilon_p > \frac{f_{yp}}{E_p}, \end{cases} \tag{15}$$

where Equation (14) represents the strain compatibility, being $\Delta\varepsilon_p$ and ε_p the strain by imposition of the prestressing system and the strain of the prestressing strand, respectively, and Equation (15) represents the stress-strain relation for the prestressing steel, being f_{yp} and E_p its yield stress and elastic modulus, respectively.

In summary, for a given value of tensile principal strain in concrete, ε_1, where such strain works as an input parameter, the shear model for the prediction of the load-deformation behavior of a

Preprints.org (www.preprints.org) | NOT PEER-REVIEWED | Posted: 3 January 2024 doi:10.20944/preprints202401.0149.v1

prestressed concrete beam is based on the nonlinear system of Equations (3-11), with to 10 equations (notice that Equation (13) is actually two equations in turn) in the 10 unknowns (θ, ε_x, ε_t, ν, ε_2, σ_2, $\sigma_{s,x}$, $\sigma_{s,t}$, ε_p and σ_p).

Equation (13) is based on the concept of forces balance between a general section (or non-cracked section, where both steel and the surrounding concrete contribute) and a cracked section (where only the reinforcement resist the internal forces; see Figure 2). The greatest value of the area A_c in order to preserve the solvability of the embedded steel constitutive model proposed by the RCFT (i.e., to preserve the internal equilibrium of forces, so that as the concrete participation increases, the steel tension decreases) is obtained by applying the following coefficient [17]:

$$\lambda = \frac{A_s \cdot f_y}{A_c \cdot f_{ct}} \cdot \left(\frac{2}{3} + \frac{\sqrt{(1 + 10.8 \cdot M \cdot \epsilon_y)^3}}{48.6 \cdot M \cdot \epsilon_y} \right), \quad (16)$$

where the coefficient λ represents the boundary of the solvability region for the embedded steel constitutive model and ϵ_y is the strain corresponding to the steel yield stress (i.e. $\epsilon_y = f_y/E_s$). For certain design cases, the previous boundary may lay within the design range prescribed by technical codes for the tension stiffening area, A_c.

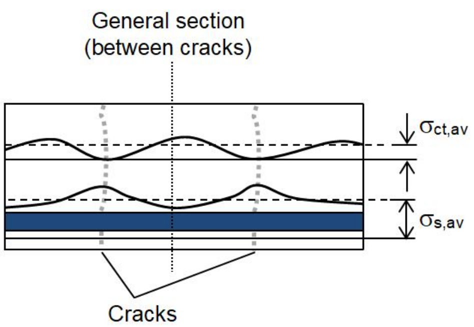

Figure 2. Average stresses profiles ($\sigma_{ct,av}$ and $\sigma_{st,av}$) for an embedded reinforcement constitutive model including several cracks.

3. Development and convergence of the method

By using the weight matrix function procedure we present a class a three-step iterative methods with the following iterative expression:

$$\begin{aligned} y^{(k)} &= x_{(k)} - [F'(x^{(k)})]^{-1} F(x^{(k)}), \\ z^{(k)} &= y^{(k)} - G(\mu^{(k)}) b [F'(x^{(k)})]^{-1} F(y^{(k)})), \\ x^{(k+1)} &= z^{(k)} - G(\mu^{(k)}) [F'(x^{(k)})]^{-1} \left(iF(z^{(k)}) + hF(y^{(k)}) \right), \; k = 0, 1, 2, \ldots \end{aligned} \quad (17)$$

where $\mu = [F'(x)]^{-1} F(y)$ is the variable of the weight function G, and b, i, and h free parameters.

On the other hand, since F is a sufficiently differentiable Fréchet function, we can regard $\xi + m \in \mathbb{R}^n$ in a neighbourhood of ξ. Using Taylor developments and $F'(\xi)$ being nonsingular,

$$F(\xi + m) = F'(\xi) \left[h + \sum_{q=2}^{p-1} C_q m^q \right] + O(m^p), \quad (18)$$

Preprints.org (www.preprints.org) | NOT PEER-REVIEWED | Posted: 3 January 2024 doi:10.20944/preprints202401.0149.v1

where $C_q = \dfrac{1}{q!}[F'(\xi)]^{-1}F^{(q)}(\xi)$, for $q \geq 2$. Also, $C_q h^q \in \mathbb{R}^n$, as $F^{(q)}(\xi) \in \mathcal{L}(\mathbb{R}^n \times \cdots \times \mathbb{R}^n, \mathbb{R}^n)$ and $[F'(\xi)]^{-1} \in \mathcal{L}(\mathbb{R}^n)$,. Therefore,

$$F(\xi + m) = F'(\xi)\left[I + \sum_{q=2}^{p-1} qC_q m^{q-1}\right] + O(m^{p-1}), \tag{19}$$

being $qC_q m^{q-1} \in \mathcal{L}(\mathbb{R}^n)$. For more details of this notation we can see [18].

Indeed, following the terms introduced by Artidiello et al. in [19], a matrix function $H : X \to X$ can be defined in such a way that its Fréchet derivatives holds

(a) $G'(u)(v) = G_1 uv$, being $G' : X \to \mathcal{L}(X)$, $G_1 \in \mathbb{R}$
a. $G''(u,v)(w) = G_2 uvw$, being $G_2 : X \times X \to \mathcal{L}(X)$, $G_2 \in \mathbb{R}$

when $X = \mathbb{R}^{n\times n}$ is the Banach space of real $n \times n$ matrices.

In the next result, we present the convergence of family (17).

Theorem 1. *Let us $F : D \subseteq \mathbb{R}^n \to \mathbb{R}^n$ be a sufficiently Fréchet differentiable function defined on an open neighborhood D of $\xi\mathbb{R}$, a zero of F. Let also be $G : \mathbb{R}^{n\times n}$ a sufficiently differentiable matrix function. Suppose that $F'(\xi)$ is nonsingular, and that $x^{(0)}$ is a seed sufficiently close to ξ. Therefore, the sequence ${x^{(k)}}_{k\geq 0}$ from (17) converges to ξ with order of convergence six if $b = \dfrac{1}{G_0}$, $h = 0$, $i = \dfrac{1}{G_0}$, $G_1 = -G_0$, and $|G_2| < \infty$, being $G_0 = G(I)$ and I the identity matrix of size $n \times n$. In this case, the error equation is*

$$\begin{aligned} e^{(k+1)} \quad = \quad & \Big(24C_2^5 - 4G_2(37C_2^5 - 6C_3 - 6C_2C_3C_2^2C_3C_2 + 3C_3C_2C_3)\frac{1}{G_0} \\ & +4G_2(32C_2^5G_0 + C_2^5G_2 - 6G_0C_3C_2^3 - 6G_0C_2C_3C_2^2 - 6G_0C_2^2C_3C_2 + 3G_0C_3C_2C_3)\left(\frac{1}{G_0}\right)^2 \\ & +2C_2^5G_0^2(3G_0 - G_2)\left(\frac{1}{G_0}\right)^3\Big) {e^{(k)}}^6 + O({e^{(k)}}^7), \end{aligned}$$

where $e^{(k)} = x^{(k)} - \xi$ and $C_q = \dfrac{1}{q!}[F'(\xi)]^{-1}F^{(q)}(\xi)$, $q = 2, 3, \ldots$

Proof. By means of the Taylor expansion of $F(x^{(k)})$ and $F'(x^{(k)})$ about ξ, we get

$$F(x^{(k)}) = F'(\xi)\left[e^{(k)} + \sum_{i=2}^{6} C_i {e^{(k)}}^i\right] + \mathcal{O}({e^{(k)}}^7),$$

and

$$F'(x^{(k)}) = F'(\xi)\left[I + + \sum_{i=2}^{5} iC_i {e^{(k)}}^{i-1}\right] + \mathcal{O}({e^{(k)}}^6).$$

We can deduce that

$$[F'(x^{(k)})]^{-1} = \left[I + + \sum_{i=2}^{5} X_i {e^{(k)}}^{i-1}\right][F'(\xi)]^{-1} + \mathcal{O}({e^{(k)}}^6),$$

where $X_2 = -2C_2$, $X_3 = -3C_3 + 4C_2^2$, $X_4 = -4C_4 + 6C_2C_3 + 6C_3C_2 - 8C_2^3$ and

$$\begin{aligned} X_5 &= -5C_5 + 8C_2C_4 - 12C_2^2C_3 + 9C_3^2 + 8C_4C_2 - 12C_2C_3C_2 + 16C_2^4 - 12C_3C_2^2, \\ X_6 &= -6C_6 + 10C_2C_5 + 12C_4C_3 - 18C_2C_3^2 - 18C_3C_2C_3 + 24C_2^3C_3 + 12C_3C_4 - 16C_2^2C_4 + 10C_5C_2 \\ &\quad - 16C_2C_4C_2 - 18C_3^2C_2 + 24C_2^2C_3C_2 - 16C_4C_2^2 + 24C_2C_3C_2^2 + 24C_3C_2^3 - 32C_2^5. \end{aligned}$$

Then,

$$\begin{aligned} y^{(k)} - \xi = {} & C_2 {e^{(k)}}^2 - 2(C_2^2 - C_3){e^{(k)}}^3 \\ & - (4C_2C_3 + 3C_3C_2 - 4C_2^3 - 3C_4){e^{(k)}}^4 \\ & - (-4C_5 + 6C_2C_4 - 8C_2^2C_3 + 6C_3^2 + 4C_4C_2 - 6C_2C_3C_2 + 8C_2^4 - 6C_3C_2^2){e^{(k)}}^5 \\ & + \mathcal{O}({e^{(k)}}^6), \end{aligned}$$

and

$$(y^{(k)} - \xi)^2 = C_2^2 {e^{(k)}}^4 + (2C_2C_3 + 2C_3C_2 - 4C_2^3){e^{(k)}}^5 + \mathcal{O}({e^{(k)}}^6).$$

Moreover,

$$\begin{aligned} F(y^{(k)}) = F'(\xi)\Big[& C_2{e^{(k)}}^2 + 2(C_3 - C_2^2){e^{(k)}}^3 + (3C_4 + 5C_2^3 - 3C_3C_2 - 4C_2C_3){e^{(k)}}^4 + \\ & (-12C_2^4 - 6C_3^2 + 4C_5 - 6C_2C_4 + 10C_2^2C_3 + 6C_3C_2^2 - 4C_4C_2 + 8C_2C_3C_2){e^{(k)}}^5\Big] \\ & + \mathcal{O}({e^{(k)}}^6). \end{aligned}$$

So,

$$\begin{aligned} F'(y^{(k)}) = F'(\xi)\Big[& I + 2C_2^2{e^{(k)}}^2 + 4(C_2C_3 - 4C_2^3){e^{(k)}}^3 + (6C_2C_4 + 8C_2^2C_3 + 3C_3C_2^2){e^{(k)}}^4\Big] \\ & + \mathcal{O}({e^{(k)}}^5). \end{aligned}$$

and

$$\begin{aligned} \mu^{(k)} = {} & -2C_2e^{(k)} + (6C_2^2 - 3C_3){e^{(k)}}^2 + (-16C_2^3 - 4C_4 + 10C_2C_3 + 6C_3C_2){e^{(k)}}^3 \\ & + (40C_2^4 + 9C_3^2 - 5C_5 + 14C_2C_4 - 28C_2^2C_3 - 15C_3C_2^2 + 8C_4C_2 - 18C_2C_3C_2){e^{(k)}}^4 \\ & + (-96C_2^5 - 6C_6 - 30C_2C_3^2 + 18C_2C_5 - 40C_2^2C_4 + 72C_2^3C_3 + 36C_3C_2^3 + 12C_3C_4 \\ & - 12C_3^2C_2 - 24C_4C_2^2 + 12C_4C_3 + 10C_5C_2 + 42C_2C_3C_2^2 \\ & - 24C_2C_4C_2 + 48C_2^2C_3C_2 - 24C_3C_2C_3){e^{(k)}}^5 + \mathcal{O}({e^{(k)}}^6). \end{aligned}$$

For the weight function G,

$$G(\mu^{(k)}) = G(I) + G_1(\mu^{(k)} - I) + \frac{1}{2}G_2(\mu^{(k)} - I)^2 + \mathcal{O}(\mu^{(k)} - I)^3,$$

that is

$$\begin{aligned} G(\mu^{(k)}) = {} & G(I) - 2C_2G_1e^{(k)} + (6C_2^2G_1 - 3C_3G_1 + 2C_2^2G_2){e^{(k)}}^2 \\ & + (-16C_2^3G_1 - 4C_4G_1 - 12C_2^3G_2 + 10G_1C_2C_3 + 3G_2C_2C_3 + 6G_1C_3C_2 + 3G_2C_3C_2){e^{(k)}}^3 + \mathcal{O}({e^{(k)}}^4). \end{aligned}$$

We denote $S = [F'(x^{(k)})]^{-1}F(y^{(k)})$. So its Taylor development can be expressed as:

$$\begin{aligned} S = {} & C_2{e^{(k)}}^2 + (-4C_2^2 + 2C_3){e^{(k)}}^3 + (13C_2^3 + 3C_4 - 8C_2C_3 - 6C_3C_2){e^{(k)}}^4 \\ & + (-38C_2^4 - 12C_3^2 + 4C_5 - 12C_2C_4 + 26C_2^2C_3 + 18C_3C_2^2 - 8C_4C_2 + 20C_2C_3C_2){e^{(k)}}^5 \\ & + \mathcal{O}({e^{(k)}}^6). \end{aligned}$$

Preprints.org (www.preprints.org) | NOT PEER-REVIEWED | Posted: 3 January 2024 doi:10.20944/preprints202401.0149.v1

So,

$$
\begin{aligned}
z^{(k)} &= (C_2 - bC_2G_0e^{(k)^2} + (-2C_2^2 + 2C_3 + 4bC_3G_0)e^{(k)^3} \\
&+ (4C_2^3 + 3G_0 - 13bC_2^3G_0 - 3bC_4G_0 - 14bC_2^3G_2 - 2bC_2^3G_2 - 4C_2C_3 \\
&+ 8bGC_2C_3 + 4bG_1C_2C_3 - 3C_3C_2 + 6bG_0C_2 + 3bG_1C_3C_2)e^{(k)^4} \\
&+ (-8C_2^4 - 6C_3^2 + 38bC_2^4G_0 + 12bC_3^2G_0 + 66bC_2^4G_1 + 6bC_3^2G_1 + 20bC_2^4G_2 + 4C_5 - 4bG_0C_5 \\
&- 6C_2C_4 + 12bG_0C_2C_4 + 6bG_1C_2C_4 + 8C_2^2C_3 - 26bG_0C_2^2C_3 - 28bG_1C_2^2C_3 - 4bG_2C_2^2C_3 \\
&+ 6C_3C_2^2 - 18bG_0C_3C_2^2 - 18bG_1C_3C_2^2 - 3bG_2C_3C_2^2 - 4C_4C_2 + 8bG_0C_4C_2 \\
&+ 4bG_1C_4C_2 + 6C_2C_3C_2 - 20bG_0C_2C_3C_2 - 22bG_1C_2C_3C_2 - 3bG_2C_2C_3C_2)e^{(k)^5} + \mathcal{O}(e^{(k)^6}).
\end{aligned}
$$

and

$$
\begin{aligned}
F(z^{(k)}) &= (C_2 - bC_2G_0)e^{(k)^2} + (-2C_2^2 + 2C_3 + 4bC_2G_0 - 2bC_3G_0 - 2bC_2^2G_1)e^{(k)^3} \\
&+ (5C_2^3 + 3C_4 - 15bC_2^3G_0 - 3bC_4G_0 + b^2c_2^3G_0^2 - 14bC_2^3G_1 - 2bC_2^3G_2 - 4C_2C_3 \\
&+ 8bG_0C_2C_3 + 4bG_1C_2C_3 - 3C_3C_2 + 6bG_0C_3C_2 + 3bG_1C_3C_2)e^{(k)^4} \\
&+ (-8C_2^4 - 6C_3^2 + 38bC_2^4G_0 + 12bC_3^2G_0 + 66bC_2^4G_1 + 6bC_3^2G_1 + 20bC_2^4G_2 + 4C_5 \\
&- 4bG_0C_5 - 6C_2C_4 + 12bG_0C_2C_4 + 6bG_1C_2C_4 + 8C_2^2C_3 - 26bG_0C_2^2C_3 - 28bG_1C_2^2C_3 \\
&- 4bG_2C_2^2C_3 + 6C_3C_2^2 - 18bG_0C_3C_2^2 - 18bG_1C_3C_2^2 - 3bG_2C_3C_2^2 - 4C_4C_2 + 8bG_0C_4C_2 \\
&+ 4bG_1C_4C_2 + 6C_2C_3C_2 - 20bG_0C_3C_2 - 22bG_1C_2C_3C_2 - 3bG_2C_2C_3C_2)e^{(k)^5} \\
&+ \mathcal{O}(e^{(k)^6}).
\end{aligned}
$$

Now, we denoted $Sc = [F'(x^{(k)})]^{-1}F(z^{(k)})$. So its Taylor expansion is:

$$
\begin{aligned}
Sc &= (C_2 - bC_2G_0)e^{(k)^2} + (-4C_2^2 + 2C_3 + 6bC_2^2G_0 - 2bC_3G_0 + 2bC_2^2G_1)e^{(k)^3} \\
&+ (13C_2^3 + 3C_4 - 27bC_2^3G_0 - 3bC_4G_0 + b^2C_2^3G_0^2 - 18bC_2^3G_1 - 2bC_2^3G_2 - 8C_2C_3 + 12bG_0C_2C_3 \\
&+ 4bG_1C_2C_3 - 6C_3C_2 + 9bGC_3C_2 + 9bG_0C_3C_2 + 3bG_1C_3C_2)e^{(k)^4} \\
&+ (-34C_2^4 - 12C_3^2 + 92bC_2^4G + 18bC_3^2G_0 - 2b^2C_2^4G_0^2 + 102bC_2^4G_1 + 6bC_3^2G_1 + 24bC_2^4G_2 + 4C_5 \\
&- 4bG_0C_5 - 12C_2C_4 + 18bG_0C_2C_4 + 6bG_1C_2C_4 + 24C_2^2C_3 - 50bG_0C_2^2C_3 - 36bG_1C_2^2C_3 \\
&- 4bG_2C_2^2C_3 + 18C_3C_2^2 - 36bG_0C_3C_2^2 - 24bG_1C_3C_2^2 - 3bG_2C_3C_2^2 - 8C_4C_2 + 12bG_0C_4C_2 \\
&+ 4bG_1C_4C_2 + 18C_2C_3C_2 - 38bG_0C_2C_3 - 28bG_1C_2C_3C_2 - 3bG_2C_2C_3C_2)e^{(k)^5} + \mathcal{O}(e^{(k)^6})
\end{aligned}
$$

Preprints.org (www.preprints.org) | NOT PEER-REVIEWED | Posted: 3 January 2024 doi:10.20944/preprints202401.0149.v1

If $Ss = iSc + hS$, then

$$
\begin{aligned}
Ss = {} & (C_2h + C_2i - bC_2Gi)e^{(k)^2} \\
& + (-4C_2^2h + 2C_3h - 4C_2^2i + 2C_3i + 6bC_2^2G_0i - 2bC_3G_0i + 2bC_2^2G_1i)e^{(k)^3} \\
& + (13C_2^3h + 3C_4h + 13C_2^3i + 3C_4i - 27bC_2^3G_0i - 3bC_4G_0i + b^2C_2^3G_0^2i - 18bC_2^3G_0i \\
& - 2bC_2^3G_2i - 8hC_2C_3 - 8iC_2C_3 + 12bG_0iC_2C_3 + 4bG_1iC_2C_3 - 6hC_3C_2 - 6iC_3C_2 \\
& + 9bG_0iC_3 + 3bG_1iC_3C_2)e^{(k)^4} \\
& + (-38C_2^4h - 12C_3h - 34C_2^4i - 12C_3^2i + 92bC_2^4G_0i + 18bC_3^2G_0i - 2bC_2^4G_0^2i + 102bC_2^4G_0i \\
& + 6bC_3^2G_0i + 24bC_2^4G_2i + 4hC_5 + 4iC_5 - 4bGiiC_5 - 12hC_2C_4 - 12iC_2C_4 + 18bGiC_2C_4 \\
& + 6bG_1iC_2C_4 + 26hC_2C_3 + 24iC_2^2C_3 - 50bG_0iC_2^2C_3 - 36bG_1iC_2^2C_3 - 4bG_2iC_2^2C_3 \\
& + 18G_0C_3C_2^2 + 18iC_3C_2^2 - 36bGiC_3C_2^2 - 24bG_1iC_3C_2^2 - 3bG_2iC_3C_2^2 - 8hC_4C_2 - 8iC_4C_2 \\
& + 12bG_0iC_4C_2 + 4bG_1iC_4C_2 + 20hC_2C_3C_2 + 18iC_2C_3C_2 - 38bGiC_2C_3C_2 - 28bG_0iC_2C_3C_2 \\
& - 3bG_2iC_2C_3C_2)e^{(k)^5} + \mathcal{O}(e^{(k)^6}).
\end{aligned}
$$

Therefore, the error equation is:

$$
\begin{aligned}
e^{(k+1)} = {} & (C_2 - bC_2G_0 - C_2G_0h - C_2G_0i + bC_2G_0^2i)e^{(k)^2} \\
& + (-2C_2^2 + 2d + 4bC_2^2G_0 - 2bdG_0 + 2bC_2^2G_0 + 4C_2^2G_0h - 2dG_0h \\
& + 2C_2^2G_0h + 4C_2^2G_0i - 2dG_0i - 6bC_2^2G_0^2i + 2bdG_0^2i + 2C_2^2G_1i - 4bC_2^2G_0G_1i)e^{(k)^3} \\
& + (4C_2^3 + 3C_4 - 13bC_2^3G_0 - 3bC_4G_0 - 14bC_2^3G_1 - 2bC_2^3G_2 - 13C_2^3G_0h - 3C_4G_0h \\
& - 14C_2^3G_1h - 2C_2^3G_2h - 13C_2^3Gi - 3C_4G_0i + 27bC_2^3G_0^2i + 3bC_4G_0^2i - b^2C_2^3G_0^3i \\
& - 14C_2^3G_1i + 36bC_2^3G_0G_1i + 4bC_2^3G_1^2i - 2C_2^3G_2ii + 4bC_2^3G_0G_2ii - 4C_2C_3 + 8bG_0C_2C_3 \\
& + 4bG_1C_2C_3 + 8G_0hC_2C_3 + 4G_1hC_2C_3 + 8G_0iC_2C_3 - 12bG_0^2iC_2C_3 + 4G_1iC_2C_3 \\
& - 8bG_0G_1iC_2C_3 - 3C_3C_2 + 6bG_0C_3C_2 + 3bG_1C_3 + 6G_0hC_3C_2 + 3G_1hC_3C_2 + 6G_0iC_3C_2 \\
& - 9bG_0^2iC_3C_2 + G_1iC_3C_2 - 6bG_0G_1iC_3C_2)e^{(k)^4} + M5e^{(k)^5} + M6e^{(k)^6} + \mathcal{O}(e^{(k)^7})
\end{aligned}
$$

Fixing $b = \dfrac{1}{G_0}$, $h = 0$, $i = \dfrac{1}{G_0}$, and $G_1 = -G_0$, the error equation becomes

$$
\begin{aligned}
e^{(k+1)} = {} & \Bigg(24C_2^5 - 4G_2(37C_2^5 - 6C_3 - 6C_2C_3C_2^2C_3C_2 + 3C_3C_2C_3)\frac{1}{G_0} \\
& + 4G_2(32C_2^5G_0 + C_2^5G_2 - 6G_0C_3C_2^3 - 6G_0C_2C_3C_2^2 - 6G_0C_2^2C_3C_2 + 3G_0C_3C_2C_3)\left(\frac{1}{G_0}\right)^2 \\
& + 2C_2^5G_0^2(3G_0 - G_2)\left(\frac{1}{G_0}\right)^3\Bigg)e^{(k)^6} + \mathcal{O}(e^{(k)^7}).
\end{aligned}
$$

With this the proof is finished. □

4. Efficiency Indices

To compare the iterative methods used, we will use the efficiency index $EI = \rho^{1/d}$, introduced by Ostrowski [20], being ρ the convergence order and d is the amount of functional evaluations, per iteration. Let us also remark that it is necessary to evaluate n scalar functions for each F and n^2 for each F'.

Preprints.org (www.preprints.org) | NOT PEER-REVIEWED | Posted: 3 January 2024 doi:10.20944/preprints202401.0149.v1

Another index for comparing different iterative schemes was introduced in [21]
In the Figure 3 we compare the computational efficiency index, CI, of several methods with Newton's method.

$$CI = \rho^{\frac{1}{(d+op)}}$$

where op is the number of products/quotients per iteration.

In each iteration five linear systems are solved with the same coefficient matrix, there are two matrix-vector products and, with respect to functional evaluations, we have two evaluations of Jacobian matrices and three of functions. The computational cost of method O6 is

$$\frac{1}{3}n^3 + 9n^2 + \frac{8}{9}n, \tag{20}$$

Table 1. Comparisons of CE

Method	CE
Newton	$2^{\frac{1}{\frac{1}{3}n^3+2n^2+\frac{2}{3}n}}$
O6	$6^{\frac{1}{\frac{1}{3}n^3+9n^2+\frac{8}{9}n}}$
PM1	$6^{\frac{1}{\frac{2}{3}n^3+11n^2+\frac{4}{3}n}}$
$M_{2,6}$	$6^{\frac{1}{\frac{2}{3}n^3+10n^2+\frac{4}{3}n}}$
$M_{6,2}(1/2,0)$	$6^{\frac{1}{\frac{1}{3}n^3+12n^2+\frac{5}{3}n}}$
FS6	$6^{\frac{1}{\frac{2}{3}n^3+10n^2+\frac{4}{3}n}}$

The results are represented in semi-logarithmic scale, see Figure 3, for a better visualization of the differences between the indices (CI), for the methods used and several sizes (n) of the systems.

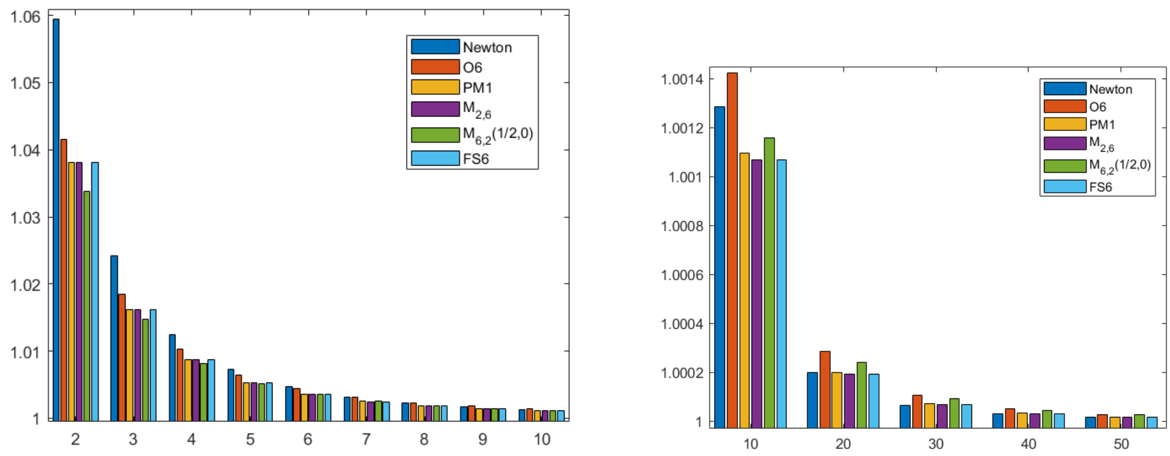

(a) Sizes from 2 to 10

(b) Sizes from 10 to 50 with a step of 10

Figure 3. Computational Efficiency Indices

In Figure 3a we can observe that, for $2 \leq n \leq 7$, the best CI index corresponds to Newton method, being O6 the best for $n > \geq 8$. In Figure 3b we can check that for bigger systems, $n \geq 10$, the best CI remains to be O6, our proposed scheme.

Preprints.org (www.preprints.org) | NOT PEER-REVIEWED | Posted: 3 January 2024 doi:10.20944/preprints202401.0149.v1

5. Numerical performance

We analyse the performance of the methods described above, to check their efficiency and compare it with other known methods The results from Tables 2 to 5 correspond to the calculations made with Matlab *R2022b*, by using variable precision arithmetics with 1200 digits of mantissa, on a PC equipped with a *Intel* Core™ i5-5200U CPU 2.20GHz. In all the tables we show the residuals $\|x^{(k+1)} - x^{(k)}\|$ and $\|F(x^{(k+1)})\|$ of the last iteration satisfying the stopping criterium $\|x^{(k+1)} - x^{(k)}\|$ or $\|F(x^{(k+1)})\|$ being lower than 10^{-300}. Moreover, a computational estimation of the order of convergence is obtained by means of ACOC introduced in [22] as

$$\rho \approx ACOC = \frac{\ln \frac{\|x^{(k+1)} - x^{(k)}\|}{\|x^{(k)} - x^{(k-1)}\|}}{\ln \frac{\|x^{(k)} - x^{(k-1)}\|}{\|x^{(k-1)} - x^{(k-2)}\|}}. \quad (21)$$

5.1. Example

We consider the nonlinear system [23]:

$$F_1(x_i) = x_i - \cos\left(2x_i - \sum_{j=1}^{4} x_j - x_i\right), i = 1, 2, 3, 4 \ldots, n, \quad (22)$$

with seed $x^{(0)} = (0.75, 0.75, \ldots, 0.75)^T$, being in this case, $\alpha \approx (0.519, 0.519, \ldots, 0.519)^T$.

In Table 2, it can be observed that the number of iterations of all the sixth-order schemes are equal and the time is very similar in all of the methods; however, the best residual is obtained by the proposed scheme O6. The ACOC estimates the theoretical order of convergence accurately, in all cases.

Table 2. Numerical results for Example 5.1

Method	Iteration	$\|x^{(k+1)} - x^{(k)}\|$	$\|F(x^{(k+1)})\|$	ρ	e-time
Newton	8	3.1586×10^{-160}	2.297×10^{-320}	2.0	0.98
O6	4	3.4133×10^{-217}	0.0	6.0	0.99
FS6	4	1.682×10^{-201}	1.614×10^{-1207}	6.0	1.02
PM1	4	6.0584×10^{-186}	4.036×10^{-1115}	6.0	0.99
$M2_6$	4	4.7636×10^{-127}	1.891×10^{-635}	5.0	1.00
$M_{6,2}(1/2,0)$	4	1.4631×10^{-189}	4.603×10^{-1137}	6.0	1.02

5.2. Example

The second example is given by [24]

$$F_2(x_i) = x_i - 2\ln\left(1 + \sum_{j=1}^{n} x_j - x_i\right), i = 1, 2, \ldots, n, \quad (23)$$

with seed $x^{(0)} = (1, 1, \ldots, 1)^T$ and $\alpha \approx (9.376, 9.376, \ldots, 9.376)^T$.

Table 3. Numerical results for Example 5.2

Method	Iterations	$\|x^{(k+1)} - x^{(k)}\|$	$\|F(x^{(k+1)})\|$	ρ	e-time (sec)
Newton	11	1.1642×10^{-199}	3.409×10^{-401}	2.0	9.99
O6	5	3.3111×10^{-100}	1.032×10^{-608}	6.0	10.24
FS6	5	5.1171×10^{-73}	1.310×10^{-445}	6.0	11.00
PM1	6	2.169×10^{-291}	3.749×10^{-1755}	6.0	10.58
$M2_6$	6	5.3026×10^{-198}	4.327×10^{-996}	6.0	11.07
$M_{6,2}(1/2,0)$	6	6.2633×10^{-289}	1.325×10^{-1206}	6.0	10.79

5.3. Example

Let us define now the nonlinear system [24],

$$F_3(x_i) = arctan(x_i) + 1 - 2\left(\sum_{n}^{j=1} x_j^2 - x_i^2\right), \tag{24}$$

with seed $x^{(0)} = (0.5, 0.5, \dots, 0.5)^T$, $n = 20$ and $\alpha \approx (0.1758, 0.1758, \dots, 0.1758)^T$.

Table 4. Numerical results for Example 5.3

Method	Iterations	$\|x^{(k+1)} - x^{(k)}\|$	$\|F(x^{(k+1)})\|$	ρ	e-time (sec)
Newton	10	1.2449×10^{-154}	1.322×10^{-307}	2.0	1.22
O6	5	1.3563×10^{-218}	2.414×10^{-1207}	6.0	1.24
FS6	4	4.4455×10^{-58}	4.283×10^{-344}	6.0	1.20
PM1	5	1.2252×10^{-218}	8.687×10^{-1208}	6.0	1.27
$M2_6$	5	6.2256×10^{-173}	5.016×10^{-861}	5.0	1.39
$M_{6,2}(1/2, 0)$	5	2.5983×10^{-252}	3.704×10^{-1208}	6.0	1.39

Let us notice in Table 4 that O6 and FS6 provide a solution satisfying the stopping criterium in less iterations as the rest of schemes. This is the reason why their residuals are not as close to zero as those of other schemes. The e-time of O6 is the second best-one.

Regarding the applied problem described in Section 2, the nonlinear shear model of a reinforced concrete beam, as its underlying data are provided by random values with few digits inside the prescribed ranges by technical standards for structural concrete; moreover, some of this parameters were fixed taking into consideration the solvability region of the adopted steel constitutive model. The stopping criterium is $\|x^{(k+1)} - x^{(k)}\|$ or $\|F(x^{(k+1)})\|$ being lower than 10^{-6}. The results provided by the new and existing schemes appear in Table 5. The ACOC does not appear in this table, as it yields to unstable data in all cases.

Table 5. Problem statement Section 2

Method	Iterations	$\|x^{(k+1)} - x^{(k)}\|$	$\|F(x^{(k+1)})\|$	e-time (sec)
Newton	5	0.0342	2.448×10^{-10}	18.3242
O6	3	9.0862	2.253×10^{-29}	21.6703
FS6	3	218.18	4.071×10^{-16}	22.1258
PM1	4	3.8554	3.138×10^{-28}	21.9594
$M2_6$	4	7.3926	9.621×10^{-21}	28.0727
$M_{6,2}(1/2, 0)$	3	0.0423	3.710×10^{-31}	22.4797

However, the best methods in terms of number of iteration are O6, FS6 and $M_{6,2}(1/2, 0)$, all with 3 iterations. Among them, the lowest e-time corresponds to our proposed scheme O6. This good performance allows us to assure the reliance and robustness of our proposed procedure.

6. Conclusions

In this article, we have developed a vectorial parametric family of numerical methods of order six, to solve a constitutive equation of reinforced concrete (6). The new class (O6) is compared to other existing methods with the same order of convergence and also with Newton's scheme. All the comparison procedures need the same or more, iterations and achieve lower precision results in the same or lower execution time, to achieve the required tolerance. This proves the accuracy, robustness and applicability of the proposed scheme.

Author Contributions: Conceptualization, , J.J.P. ; methodology, F.I.C..; software, A.C.and F.I.C.; formal analysis, J.R.T.; investigation, A.C. ; writing—original draft preparation, J.J.P. and A.M.H.; writing—review and editing, A.C. and J.R.T. All authors have read and agreed to the published version of the manuscript.

Funding: No funding.

Institutional Review Board Statement: Not applicable

Informed Consent Statement: Not applicable

Data Availability Statement: Not applicable

Conflicts of Interest: The authors declare no conflict of interest.

References

1. Collins, M.P.; Mitchell, D. *Prestressed concrete structures*; Vol. 9, Prentice Hall Englewood Cliffs, NJ, 1991.
2. on Shear, A.A.C..; Torsion. Recent approaches to shear design of structural concrete. *Journal of structural engineering* **1998**, *124*, 1375–1417.
3. Galántai, A. The theory of Newton's method. *Journal of Computational and Applied Mathematics* **2000**, *124*, 25–44.
4. Hernández-Díaz, A.M.; Bueno-Crespo, A.; Pérez-Aracil, J.; Cecilia, J.M. Multi-objective optimal design of submerged arches using extreme learning machine and evolutionary algorithms. *Applied Soft Computing* **2018**, *71*, 826–834.
5. A.M. Hernández-Díaz, A. Muñoz, J.J.A.; Sáez, A. Buckling design of submerged arches via shape parameterization. *Computational and Mathematical Methods* **2019**, *1*, e1057.
6. J.F. Jiménez-Alonso, J. Pérez-Aracil, A.H.D.; Sáez, A. Effect of Vinyl flooring on the modal properties of a steel footbridge. *Applied Sciences* **2019**, *9*, 1374.
7. J. Pérez-Aracil, C. Camacho-Gómez, A.H.D.; E. Pereira, D.C.; Salcedo-Sanz, S. Memetic coral reefs optimization algorithms for optimal geometrical design of submerged arches. *Swarm and Evolutionary Computation* **2021**, *67*, 100958.
8. Hueso, J.L.; Martínez, E.; Teruel, C. Convergence, efficiency and dynamics of new fourth and sixth order families of iterative methods for nonlinear systems. *Journal of Computational and Applied Mathematics* **2015**, *275*, 412–420.
9. Narang, M.; Bhatia, S.; Kanwar, V. New two-parameter Chebyshev–Halley-like family of fourth and sixth-order methods for systems of nonlinear equations. *Applied Mathematics and Computation* **2016**, *275*, 394–403.
10. Behl, R.; Maroju, P.; Motsa, S. Efficient family of sixth-order methods for nonlinear models with its dynamics. *International Journal of Computational Methods* **2019**, *16*, 1840008.
11. Yaseen, S.; Zafar, F. A new sixth-order Jarratt-type iterative method for systems of nonlinear equations. *Arabian Journal of Mathematics* **2022**, *11*, 585–599.
12. Vecchio, F.J.; Collins, M.P. The modified compression-field theory for reinforced concrete elements subjected to shear. *ACI J.* **1986**, *83*, 219–231.
13. Hernández-Dı, A.; Gil-Martı, L.; others. Analysis of the equal principal angles assumption in the shear design of reinforced concrete members. *Engineering structures* **2012**, *42*, 95–105.
14. Belarbi, A.; Hsu, T. Constitutive laws of concrete in tension and reinforcing bars stiffened by concrete. *Structural Journal* **1994**, *91*, 465–474.
15. L.M. Gil-Martín, L. María, E.H.M.; Aschheim, M.; Pantazopoulou, S. Refinements to compression field theory, with application to wall-type structures. *American Concrete Institute Special Publication* **2009**, *265*, 123–142.
16. M. Palermo, L.M. Gil-Martin, E.H.M.; Aschheim, M. Refined compression field theory for plastered straw bale walls. *Construction and Building Materials* **2014**, *58*, 101–110.
17. A.M.Hernández-Díaz.; García-Román, M. Computing the refined compression field theory. *International Journal of Concrete Structures and Materials* **2016**, *10*, 143–147.
18. Cordero, A.; Hueso, J.L.; Martínez, E.; Torregrosa, J.R. A modified Newton-Jarratt's composition. *Numer. Algor.* **2010**, *55*, 87–99.

19. Artidiello, S.; Cordero, A.; Torregrosa, J.R.; Vassileva, M.P. Multidimensional generalization of iterative methods for solving nonlinear problems by means of weight-function procedure. *Applied Mathematics and Computation* **2015**, *268*, 1064–1071.
20. A.M., O. *Solutions of equations and systems of equations*; Academic Press, New York, 1966.
21. Cordero, A.; Torregrosa, J.R. On interpolation variants of Newton's method for functions of several variables. *Journal of Computational and Applied Mathematics* **2010**, *234*, 34–43.
22. Cordero, A.; Torregrosa, J. Variants of Newton's method using fifth-order quadrature formulas. *Applied Mathematics and Computation* **2007**, *190*, 686–698.
23. Artidiello, S.; Cordero, A.; Torregrosa, J.R.; Vassileva, M.P. Design and multidimensional extension of iterative methods for solving nonlinear problems. *Applied Mathematics and Computation* **2017**, *293*, 194–203.
24. Cordero, A.; Jordán, C.; Sanabria, E.; Torregrosa, J.R. A new class of iterative processes for solving nonlinear systems by using one divided differences operator. *Mathematics* **2019**, *7*, 776.